Available online at www.sciencedirect.com
ScienceDirect
Journal of Catalysis 253 (2008) 191–199
JOURNAL OF CATALYSIS
www.elsevier.com/locate/jcat

Molecular traffic control for a cracking reaction

R. Harish [a,b,*], D. Karevski [c], G.M. Schütz [a]

[a] *Institut für Festkörperforschung, Forschungszentrum Jülich, 52425 Jülich, Germany*
[b] *Reactor Physics Division, Indira Gandhi Centre for Atomic Research, Kalpakkam 603102, India*
[c] *Laboratoire de Physique des Matériaux, Université Henri Poincaré, Nancy I, Nancy Cedex, France*

Received 17 May 2007; revised 10 September 2007; accepted 12 October 2007

Available online 26 November 2007

Abstract

We investigate the conditions for reactivity enhancement of a catalytic cracking process in porous crystalline solids using the concept of molecular traffic control (MTC). Using dynamic Monte Carlo simulations we obtain a quantitative description of the MTC effect for a bimodal network of intersecting size-selective channels over a wide range of grain parameters, diffusivities and reaction constants, and external operating conditions. The results are compared with those obtained on a similar network but with only one type of channels, called the reference system. We find significant reactivity enhancement in the MTC system with respect to the reference system. This effect is observed to increase with the grain size, and also with longer segments between lattice intersections. We find that in certain regions of the microscopic reaction rate the reactivity enhancement is up to 68%.
© 2007 Elsevier Inc. All rights reserved.

Keywords: Molecular traffic control; Dynamic Monte Carlo simulation; Cracking; Zeolites; Reactivity enhancement

1. Introduction

Zeolites are used for a variety of industrial applications, e.g., isomerization and cracking of hydrocarbons in the petroleum industry [1,2]. In a number of zeolites diffusive transport takes place in quasi one-dimensional channels where the guest molecules may block the movement of each other [3]. Due to mutual blockage of reactant and product molecules under such *single file conditions* [4], the effective reactivity of a catalytic process (which is determined by the residence time of molecules inside the zeolite) may be considerably reduced as compared to the reactivity in the absence of single file behaviour. This results in a very low output of product molecules from the catalytic grain. In order to overcome this problem, the concept of molecular traffic control (MTC) was suggested [5,6]. In MTC one has spatially separated pathways for the reactant and product molecules. This avoids the mutual suppression of self diffusion in the grains and thus reduces the residence time. The concept of MTC has remained controversial for a long time.

To test whether the MTC effect leads to enhancement of grain reactivity, several authors have carried out dynamic Monte Carlo simulations (DMCS) of a stochastic model system with a two-dimensional network of perpendicular sets of bimodal intersecting pore channels and catalytic sites located at the intersections of the pores [7–12], referred to as the NBK model. The authors of these papers studied numerically the occurrence of the MTC effect by comparing the outflow of reaction products in the MTC system with a reference system (REF) which is identical to the MTC system but with only one type of channels carrying both the reactant and product particles.

An MTC effect in the NBK topology was found, and turned out to be favoured by a small number of channels and long channel segments between intersections, which by themselves lead to a very low absolute outflow compared to a similar system with shorter channel segments. For reasonable reactivities and moderate channel segment lengths, the MTC effect is inversely proportional to the grain diameter [11] and vanishes already for rather small lattices. Extension of the topology to three dimensions leads to similar results, suggesting that an appreciable MTC effect can occur, but only in tiny nanometer-sized crystallites [12]. With a view on exploiting the MTC effect in commercially used zeolite grains this observation ne-

* Corresponding author. Fax: +91 44 27480104.
E-mail addresses: harish@igcar.gov.in, harish_juelich@yahoo.co.in (R. Harish).

0021-9517/$ – see front matter © 2007 Elsevier Inc. All rights reserved.
doi:10.1016/j.jcat.2007.10.009

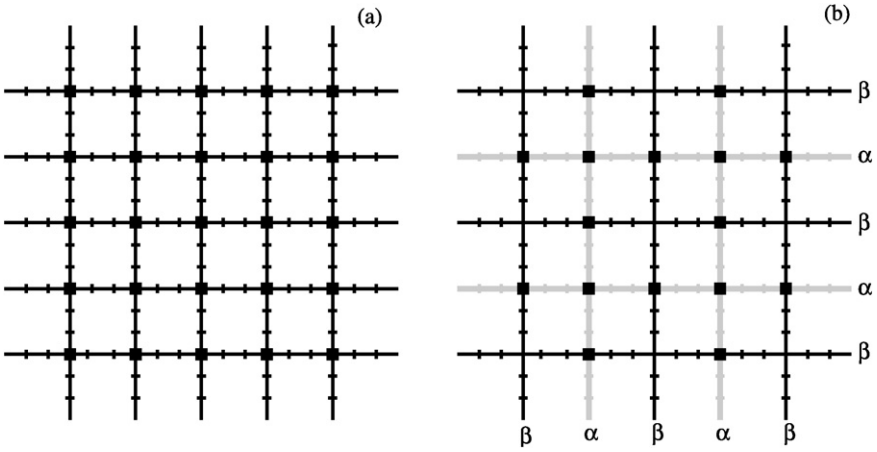

Fig. 1. REF system (a) and MTC system with BrS topology (b). In (a) all the channels carry both A- and B-particles. In (b), the channels which carry only the product B-particles (β-channels) are shown in black and the channels which carry both A- and B-particles (α-channels) are shown in gray. Intersections where the catalytic reactions are possible are marked with a solid square. The end sites of the channels are the reservoir sites. The lattice is $N \times N$ ($N = 5$) with two sites between intersections ($L = 2$).

cessitates searching for alternative MTC topologies which in principle would work for grains of any size. To this end, a new two-dimensional bimodal channel topology was proposed, where the channels are alternately placed in both the directions [13], see Fig. 1. This channel topology is subsequently referred to as BrS topology.

A series of DMCS for this topology has shown that indeed the grain reactivity is enhanced for larger grains at some system parameters. This will be useful in applications where large porous solids having lattice networks identical to or similar to the BrS topology are used. Recently the zeolite material TNU-9 has been characterized [14]. The structure consists of parallel layers (y–z plane), with two types of channels of different sizes (say α and β) alternately placed along the y-direction, α-channels placed along the z-direction and the parallel layers connected by the β-channels (see [14] for details). The two-dimensional BrS topology along both the directions resembles the TNU-9 structure along the y-direction.

All the theoretical studies of MTC in zeolites so far consider the *isomerization* reaction $A \to B$, which is a conversion of a reactant molecule A to a product molecule B, under single file conditions. In these studies it is assumed that A- and B-molecules have the same diffusion rates. Two cases are studied, shape selectivity and size selectivity. In the case of shape selectivity, the reactant and product molecules diffuse in different channels (α- and β-channels, respectively defined in Fig. 1). In the case of size selectivity, the reactant molecules diffuse only in the α-channels, whereas the product molecules diffuse in both α- and β-channels. The behaviour of the stationary outflow of B-molecules is qualitatively similar in both the cases. However, if the product molecules are smaller in size as compared to the reactant molecules, the more realistic case would be the size selectivity case, as both reactant and product molecules can diffuse through the α-channels. We note that in all studies of the NBK-model only shape-selectivity was considered.

Our aim is to study a *cracking* reaction in the BrS topology, with a combination of single-file conditions and size-selectivity in a bimodal channel system. Moreover, we wish to investigate the strength of the MTC effect for different diffusion rates of reactant and product molecules. In the following, we report simulation results of a cracking reaction in the BrS topology, which is an important reaction from the point of application, where we assume that an A-molecule gets cracked to two B-molecules.

The paper is organized as follows. In Section 2 we describe the lattice system and the model used for simulation. In Section 3 we present our results. First, we describe the dynamic Monte Carlo algorithm used (Section 3.1). Then, we present some analytical results obtained for the molecular outflow for a lattice with one intersection (Section 3.2). In Section 3.3 we present the results of Monte Carlo (MC) simulations; for equal diffusion rate for both reactant and product particles (Section 3.3.1), and when the diffusion rate of the product molecules is varied (Section 3.3.2). Finally we present a summary in Section 4.

2. Model

We consider a cracking reaction $A \to 2B$ in a catalytically active porous grain, surrounded by a gas phase to which A-molecules are supplied at constant rate and from which B-molecules are constantly extracted. By studying a reaction–diffusion process on a *molecular* scale inside a catalytic grain we encounter local concentration gradients inside the grain which are maintained by the constant supply of reactants and removal of reaction products and which thus drive the system into a strongly nonequilibrium steady state.

There is no quantitative theory to estimate the outflow or the density profiles of the reactant and product molecules inside the grain under such circumstances and hence it is necessary to take recourse to numerical methods. Being faced with a stationary process far from thermal equilibrium excludes a description both by molecular dynamics simulation and by usual equilibrium Monte Carlo techniques. Instead we adapt earlier work to our present problem and choose an approach amenable to numerical treatment by means of dynamical Monte Carlo sim-

ulation (DMCS) [10–13,15]. A detailed review of modeling of diffusion in zeolites is given in [16].

The main quantity of interest is the stationary molecular flow of B-molecules into the gas phase as this quantity measures the effective reactivity of a catalytic grain. In the lattice gas description adopted in the Monte Carlo model described below molecules of type A or B are described by particles without internal structure. Correspondingly the molecular flow is proportional to the output *current* of B-particles. This is the (stationary) average number of B-particles that leave the grain per time unit. Since we are interested in comparing the outflow of two different models, the MTC system and the reference system, the actual time unit is immaterial as it cancels in the efficiency ratio defined below. When referring to the model in the technical part of the paper we shall use the expression current rather than molecular flow and particle rather than molecule.

For the MTC-grain we use BrS topological model with a quadratic array of $N \times N$ channels which is a measure of the grain size (Fig. 1b). We assume the lattice to be embedded in a reservoir of A- and B-particles which represents the gas phase surrounding the grain. The sites next to the reservoir where molecules from the gas phase can enter and leave the grain are called the boundary sites. Each channel has L sites between the intersection points or between an intersection and the reservoir.

A- and B-particles diffuse inside the channels or between the boundary sites and the reservoir by attempting to hop to the adjacent site with rate D_A (D_B). Whether a hopping attempt is successful or not depends on whether the target site is allowed to be filled or not. The binary channel structure is assumed to be size-selective with the simplifying assumption on the microscopic pore structure that A-particles are allowed to enter only the α-channels, whereas B-particles are allowed to enter both the α- and β-channels. More precisely, we assume that the entrances of the β-channels are small enough so that A-particles do not enter them, yet the interior of the β-channels is large enough to allow two B-particles to be occupied by a lattice site. Generally hard-core repulsion is assumed between A and A and between A- and B-particles, such that if a lattice site is occupied by one A-particle it may not be occupied by another particle of any type (exclusion rule). On the other hand, since two B-particles are created at the expense of one A-particle, we relax the exclusion rule for B-particles and assume that any lattice site in the α-channel is either empty or allowed to be occupied by one A-particle, or at most two B-particles. In a β-channel, a lattice site is empty or is allowed to be occupied by one B-particle or (at most) two B-particles. The cracking reaction is allowed to take place only at the intersections accessible to the A-particles with rate c, where an A-particle is annihilated and two B-particles are created.

At the boundary sites, A- and B-particles are injected into the lattice with rates $D_A\rho_A$ and $D_B\rho_B$, respectively. Since the reaction product B is constantly removed from the gas phase we assume that the reservoir consists entirely of A-particles and therefore set $\rho_B = 0$. Because of size selectivity it is also assumed that the reservoir sites at the end of the β-channels cannot be occupied by A-particles. Therefore there is no particle injection at the boundaries of β-channels. At the boundaries of α-channels A- and B-particles jump into the reservoir with rates $D_A(1-\rho_A)$ and $D_B(1-\rho_A)$, respectively. At the boundaries of β-channels B-particles jump with rate D_B into the reservoir. Notice that jump attempts into the reservoir with the given rates are always successful and amount to annihilation of particles from the boundary sites with the respective jump rates. This boundary-reservoir dynamics which describes the exchange of particles between the grain and the surrounding gas phase is equivalent to representing the gas phase by a reservoir site which is occupied at all times by an A-particle with probability ρ_A and then letting particles attempt to jump between reservoir site and boundary site with rates $D_{A,B}$ as in the bulk.

The results for the MTC for the BrS topology are compared with a reference (REF) system, where all the channels are α-channels, i.e., all the channels allow diffusion of both A- and B-particles in them and have exchange with the reservoir as discussed above for α-channels. Catalytic cracking occurs at all intersection sites.

To be precise we remark that in the mathematical model described above all transition attempts are assumed to occur in continuous time. These are Poisson processes which take place after an exponentially distributed random time, the inverse mean of which is the attempt rate. An exponentially distributed random time is a standard assumption expected from the theory of thermally activated processes.

3. Monte Carlo results

For numerical simulation of the model described above we adopt the dynamic Monte Carlo algorithm with random sequential update for the calculation of the current of B-particles [16].

First we describe in some detail the algorithm (Section 3.1). Then the simulation results obtained for a lattice with one intersection are compared with exact analytical results and the comparison is found to be very good (Section 3.2). The numerical results for larger lattices are reported in Section 3.3. We are mainly interested in the stationary current of B-particles from the lattice per unit time, i.e., the number of B-particles that are absorbed by the reservoir from the boundary sites per unit time.

3.1. Algorithm

Since $\rho_B = 0$, B-particles that hop to the reservoir site are removed from it immediately. For simulating hopping and reaction events of the process, we first choose a bond connecting two adjacent lattice sites. Each bond is chosen randomly with equal probability. As a technical point we remind the interested reader that the random sequential update discretizes time into small units of approximately the order of the inverse number of lattice sites and thus replaces the exponential distribution of random times underlying the definition of the continuous-time process introduced above by a geometric distribution. Thus an exponential sojourn probability $s(t) = \exp(-xt)$ for some process with transition rate x is simulated by a sojourn probability $\tilde{s}(x) \approx (1 - x/M)^{Mt}$, where M is the (large) number of bonds in our lattice model.

Then the hopping rates D_A, D_B, and the reaction rate c are converted to the respective probabilities for hopping $\tilde{D}_A$, $\tilde{D}_B$, and reaction $\tilde{c}$. The probabilities are proportional to the rates:

$$\tilde{D}_A = \eta D_A, \qquad \tilde{D}_B = \eta D_B, \qquad \tilde{c} = \eta c. \tag{1}$$

It follows that

$$\frac{\tilde{D}_A}{\tilde{c}} = \frac{D_A}{c}, \qquad \frac{\tilde{D}_B}{\tilde{c}} = \frac{D_B}{c},$$
$$0 \leqslant \tilde{D}_B \leqslant 1, \qquad 0 \leqslant \tilde{D}_A + \tilde{c} \leqslant 1. \tag{2}$$

The last condition in (2) is to ensure that at most a hopping of an A-particle or a cracking reaction takes place when a bond connected to an α–α or α–β intersection is chosen. For the case, $D_A \geqslant D_B$, one can choose $\tilde{c} + \tilde{D}_A = 1$, so as to maximize the efficiency of the algorithm. The constant of proportionality η in Eq. (1) is given by

$$\eta = \frac{1}{D_A + c} \quad \text{for } D_A \geqslant D_B,$$
$$\eta = \frac{D_A}{D_B(D_A + c)} \quad \text{for } D_A < D_B. \tag{3}$$

To implement an event associated with the bond, next a random number r between 0 and 1 is drawn from a uniform distribution. There exist four types of bonds: (1) bonds in a channel, (2) bonds connected to β–β intersections, (3) bonds connected to α–α or α–β intersections, and (4) bonds connected to the reservoir (i.e., bond between a boundary site and its associated reservoir site).

(1) If the bond is a channel bond a hopping direction is chosen randomly with equal probability. Then hopping across the bond by one particle is attempted. If a hop is allowed, as discussed in Section 2, it is implemented with the corresponding probability. The hopping possibilities are tabulated in Table 1.
(2) The procedure for implementing hops across bonds connected to β–β intersections is the same as that for channel bonds as the cracking reaction cannot take place on this bond.
(3) If the chosen bond is connected to an α–α or α–β intersection, then
   - if the intersection is occupied by an A-particle and $0 < r < \tilde{c}$, replace A by $2B$ at the intersection,
   - otherwise treat it as a channel bond and follow the procedure as for a channel bond.
(4) If the chosen bond is connected to a reservoir site follow the same procedure as for a channel bond and then
   - if the bond is in an α-channel, fill the reservoir site with an A-particle with probability ρ_A, irrespective of the occupation after the jump attempt,
   - if the bond is in a β channel, delete the B-particle in the reservoir site, if there is one.

If a B-particle has hopped to the reservoir site then the current counter $i(B) = i(B) + 1$ is incremented.

If no event is possible on the chosen bond, choose another bond randomly and repeat. The procedure is repeated M times, called an MC update, where M is the number of bonds in the lattice.

Table 1
Hopping transitions and their probabilities

Configuration	Transition	Probability
0–A or A–0	0–A → A–0 or A–0 → 0–A	$\tilde{c} < r < \tilde{c} + \tilde{D}_A$
0–B or B–0	0–B → B–0 or B–0 → 0–B	$0 < r < \tilde{D}_B$
B–2B or 2B–B	B–2B → 2B–B or 2B–B → B–2B	$0 < r < \tilde{D}_B$
2B–0 or 0–2B	2B–0 → B–B or 0–2B → B–B	$0 < r < \tilde{D}_B$
B–B	B–B → 2B–0	$0 < r < \tilde{D}_B/2$
B–B	B–B → 0–2B	$\tilde{D}_B/2 < r < \tilde{D}_B$

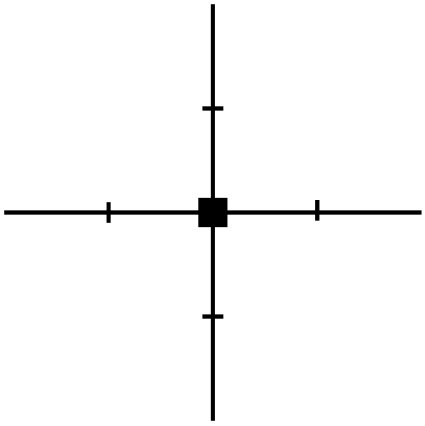

Fig. 2. Model for one intersection with four channel segments. The end sites of the channels are the reservoir sites. One lattice site between the intersection and the reservoir site is shown.

The procedure is carried out a large number of times T. After T MC updates, a new initial condition is chosen and further T MC updates are carried out. This procedure is carried out for E number of initial conditions, so as to remove any dependence on the initial conditions. The initial condition for the lattice is set up by filling the reservoir sites of the α-channels with A-particles according to ρ_A: a given reservoir site is filled by an A-particle with probability ρ_A. E and T should be chosen such that the current $j(B)$ obtained is stationary. The current $j(B)$ is calculated at time T as

$$j(B) = i(B)/(\eta T E). \tag{4}$$

We have found $T = 2000$ MC steps to give good stationarity of the current when averaged over an ensemble size of $E = 2000$. For the simulations we chose ran2 as the random number generator [17]. The statistical errors are small and the error bars are within the symbol size and not plotted. We refer to the rates and not probabilities in the following and also set $\rho = \rho_A$ since $\rho_B = 0$.

3.2. Analytical results for one intersection

In this section we consider the situation of one intersection connected to the reservoir through n channel segments with one site per channel (see Fig. 2 for $n = 4$, in the nomenclature of Fig. 1, $N = 1$, $L = 1$).

The cracking reaction $A \to 2B$ is assumed to take place instantaneously when an A-particle reaches the intersection site,

which implies $c = \infty$. Consequently, the intersection site is empty, occupied by either one B-particle or two B-particles, while the external sites are empty, occupied by one A-particle, one B-particle or two B-particles. The evolution of the probability $P(x,t)$ of finding the system in a configuration x at time t is governed by the master equation:

$$\partial_t P(x,t) = \sum_{y\neq x}\big\{w(y\to x)P(y,t) - w(x\to y)P(x,t)\big\}, \quad (5)$$

where $w(y\to x)$ are the transition rates for the system to change its configuration from state y to state x per unit time. The first sum of the r.h.s. of Eq. (5) represents the incoming flux into state x while the second sum represents the outgoing flux from state x. In the stationary state, the time derivative in Eq. (5) vanishes and one obtains the balance equation

$$\sum_{y\neq x} w(y\to x)P^*(y) = \sum_{y\neq x} w(x\to y)P^*(x), \quad (6)$$

where $P^*(x)$ is the stationary probability distribution. In the steady state one can write down the balance equations in terms of the correlation functions associated with the system.

In the REF system (Fig. 2), due to the symmetry of the problem, the three types of possible correlation functions are:

$$\begin{aligned} E_{jkl} &= \langle \underbrace{A\ldots A}_{j}\,\underbrace{B\ldots B}_{k}\,\underbrace{C\ldots C}_{l}\rangle,\\ B_{jkl} &= \langle B_0\,\underbrace{A\ldots A}_{j}\,\underbrace{B\ldots B}_{k}\,\underbrace{C\ldots C}_{l}\rangle,\\ C_{jkl} &= \langle C_0\,\underbrace{A\ldots A}_{j}\,\underbrace{B\ldots B}_{k}\,\underbrace{C\ldots C}_{l}\rangle. \end{aligned} \quad (7)$$

Here, C represents $2B$ particles on a site, E_{jkl} represents configurations with j number of A-particles, k number of B-particles, and l number of C-particles on the lattice with the intersection site being empty. B_{jkl} and C_{jkl} are defined similarly but with B_0 and C_0 as the occupation probability of the intersection site (see Fig. 3). However, in the MTC system, one has to distinguish between α- and β-channels.

In the following we set $D_A = 1$ which fixes the time scale. In the REF system, for the incoming contribution E_{jkl} correlator is given by

$$\begin{aligned} &j\rho[E_{j-1kl} - E_{jkl} - E_{j-1k+1l} - E_{j-1kl+1}]\\ &\quad + D_B k[B_{jk-1l} - B_{j+1k-1l} - B_{jkl} - B_{jk-1l+1}\\ &\quad + C_{jk-1l} - C_{j+1k-1l} - C_{jkl} - 2C_{jk-1l+1} + E_{jk-1l+1}]\\ &\quad + D_B k(1-\rho)E_{jk-1l+1} + D_B l C_{jk+1l-1}\\ &\quad + \frac{1}{2}D_B l B_{jk+1l-1}, \end{aligned} \quad (8)$$

which has to be balanced in the steady state by the outgoing contribution,

$$(2-\rho)\big[j + D_B(k+l)\big]E_{jkl} - jB_{jkl} - [D_B l + j]C_{jkl}. \quad (9)$$

One may write down similar equations for the B_{jkl} and C_{jkl} correlators and the set of coupled linear equations can be solved, for example using Maple. The current of B-particles per channel segment is given by

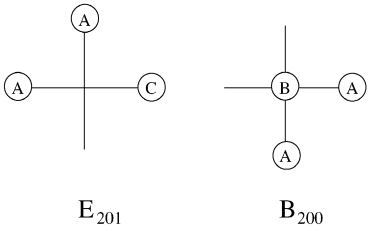

Fig. 3. Correlation functions $E_{201} = \langle AAC\rangle$ and $B_{200} = \langle B_0 AA\rangle$.

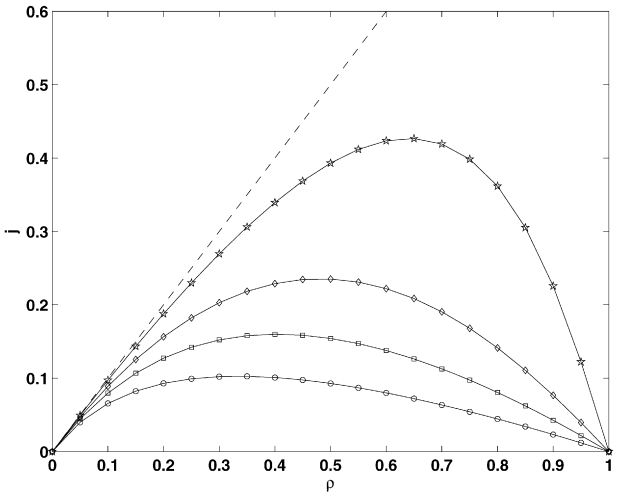

Fig. 4. Current j per channel segment for the one intersection model with diffusion rate $D_A = 1$ and for diffusion rates $D_B = 1/2$ (○), $D_B = 1$ (□), $D_B = 2$ (◇), and $D_B = 8$ (★). The dashed line $j = \rho$ corresponds to the limiting case $D_B \to \infty$.

$$j_B = 2\langle V_0 A\rangle = 2(E_{100} - B_{100} - C_{100}), \quad (10)$$

where V_0 stands for a vacancy at the intersection.

In Fig. 4 we have plotted the current j as a function of ρ for different diffusion rates D_B. One observes that as the B-particle diffusion rate increases the maximum current shifts to the right. The current is almost symmetric for $D_B = 2$. As $D_B \to \infty$, $j \to \rho$ which is shown as the dashed line. It is seen that for moderate D_B and for small values of ρ, the current is close to the infinite diffusion rate line. In Table 2 we present a comparison of our MC simulation results obtained for a reaction rate of $c = 100$ with the exact results of the infinite reaction rate case. The MC data are given for the total B-particle current (which is 4 times the current for the single segment since we have 4 channel segments in the REF system). Almost all deviations from the analytical values are less than 1%.

In Fig. 5 we present the exact results obtained for the case where an intersection is connected to the reservoir by two channel segments: in the REF system both the channel segments are α-channel segments and for the MTC case, one is an α-channel segment and the other is a β-channel segment. It is seen that the current in the MTC system is less than that in the REF system when the reservoir density ρ is small. As ρ is increased the α-channels get increasingly blocked resulting in decreased current eventually tending to zero in the REF case. On the other hand, in the MTC system, this results in an increased motion of A-particles toward the intersection and as the β-channels are

Table 2
Comparison of MC and exact results of the total current for the single intersection for $D_A = D_B = 1$

ρ	MC	Exact	% deviation
0.1	0.3191	0.3184	0.22
0.2	0.5135	0.5096	0.77
0.3	0.6089	0.6088	0.01
0.4	0.6381	0.6392	0.17
0.5	0.6157	0.6168	0.17
0.6	0.5520	0.5512	0.14
0.7	0.4477	0.4504	0.60
0.8	0.3230	0.3216	0.43
0.9	0.1685	0.1704	1.11

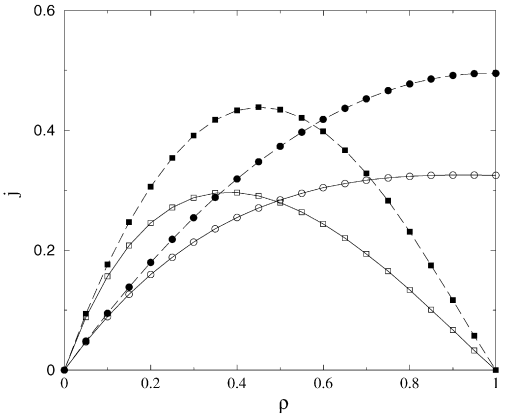

Fig. 5. Total B-particle current j for the one intersection case (two channel segments) for $D_A = 1$. $D_B = 1$ REF (□), $D_B = 2$ REF (■), $D_B = 1$, MTC (○), and $D_B = 2$ MTC (●).

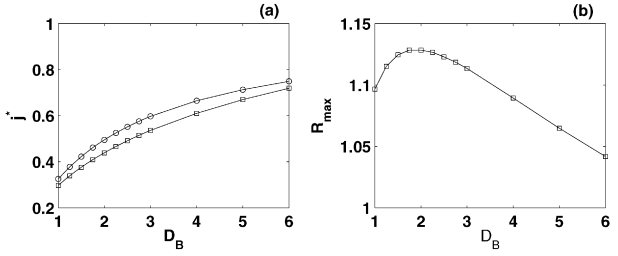

Fig. 6. Maximum current j^* for the one intersection (two channel segments) case $D_A = 1$, REF (□) and MTC (○) as a function of D_B (a). The maximum efficiency ratio as a function of D_B (b).

available for the exit of B-particles, the current monotonically increases. This is evident in Fig. 5. We also note that for the values of D_B considered, the maximum current with respect to ρ is higher for MTC system than for the REF system, which is clearly an MTC effect. We also note that the MTC effect is observed at higher values of ρ as D_B is increased.

In Fig. 6a we have plotted the maximum current j^* (w.r.t. ρ) for both REF and MTC systems. It can be seen that there is always a MTC effect for all values of D_B. In Fig. 6b, we have plotted the maximal efficiency ratio

$$R = \frac{j^*_{\mathrm{MTC}}}{j^*_{\mathrm{REF}}} \tag{11}$$

as a function of D_B. It presents a maximum around $D_B = 2$ and then decreases toward unity as the mobility of B-particles

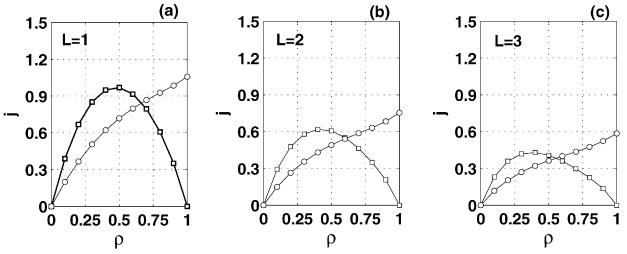

Fig. 7. Current j for the REF system (□) and MTC (○) for a system of 5×5 ($N = 5$) channels for $c = 0.05$, $D_A = 0.5$, and $D_B = 0.5$. The current for both REF and MTC systems decreases with L. Efficiency ratio R increases with L.

increases. One may notice that the behaviour obtained already in the 2 channel segment case seems to be quite generic as seen from the MC results presented in the next section.

3.3. Numerical results for large lattices

We wish to calculate the current of B-particles from the lattice immersed in a reservoir of A-particles of density ρ. The purpose is to study the current as a function of the hopping rates D_A, D_B, and the reaction rate c in the BrS topology for lattice sizes determined by N and L and compare it with the REF system to evaluate the MTC effect in the BrS topology for the cracking reaction.

3.3.1. $D_A = D_B$

First, we consider the case when the diffusion rates for the reactant and product particles are the same. In Fig. 7 the output current from the REF and MTC lattice are presented for a network of 5×5 channels ($N = 5$) with the number of sites L between intersections ranging from 1 to 3 for $D_A = D_B = 0.5$ and $c = 0.05$. As the A-particles start blocking the boundary sites of the α-channels for increasing values of the reservoir density ρ, the current tends to 0 as the density ρ approaches unity for the REF system. On the other hand, the β-channels are available for exit of B-particles in MTC case so that monotonicity of current with ρ is observed. This is in accordance with the one intersection case (cf. Fig. 5). The current for both REF and MTC systems decreases substantially with length between intersections L which is in qualitative agreement with the results of [10,13]. For single file systems, it can be shown theoretically that the current in the REF system is proportional to L^{-2} and in the MTC system it is proportional to L^{-1} [10] in a channel. Although the reaction–diffusion mechanism is somewhat different in our case (combination of exclusion and nonexclusion dynamics due to different size of A- and B-particles), we find qualitatively the same behaviour as in the isomerization case where A- and B-particles are of similar size (modeled by full exclusion for each species of molecules).

Generally, the currents decrease with increasing values of L. The current drops by a factor of nearly three in the REF case whereas in the MTC system the drop is by a factor of nearly two as L is increased from $L = 1$ to $L = 3$. This is reflected very clearly in terms of the efficiency ratio R defined in Eq. (11), where we observe almost a 30% increase in the MTC system. Numerical results for the isomerization reaction where both A-

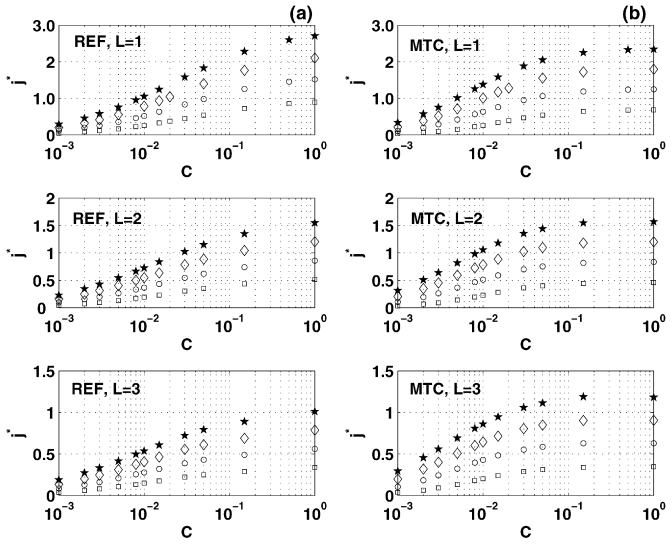

Fig. 8. Maximal current j^* for REF (a) and MTC (b) for $N = 3$ (□), $N = 5$ (○), $N = 7$ (◇), and $N = 9$ (★) for $D_A = D_B = 0.5$.

and B-particles are allowed in the α-channel (partial shape selectivity) also exhibit monotonic behaviour of R with L [13], although the MTC effect is less pronounced. Our size-selective model shows similar quantitative behaviour [13]. For the isomerization with partial shape selectivity ($L = 2$), the efficiency ratio is $R = 1.19$ [13], whereas in the present case, we have $R = 1.22$. The slight increase in the present case may be due to the ability of the B-particles to pass each other in the β-channels.

Fig. 8 shows the maximal current j^* for the REF system for the reaction rate ranging from $c = 0.001$ to $c = 1.0$. The maximal value of the current occurs in the REF case at some value strictly between 0 and 1, see Fig. 7. It is obtained as the maximum of a polynomial fit (up to degree 4) for $j(\rho)$. For both the systems the currents are plotted for $N = 3, 5, 7, 9$ for $L = 1, 2, 3$. In the REF system, Fig. 8a, for small values of c, the current appears to increase logarithmically. For higher values of c, which implies complete cracking of A-particles into two B-particles, the current approaches its maximum value. As expected from theoretical considerations discussed above, the maximal current decreases when L is increased. The maximal current also increases linearly with N as the number of intersections increases where the cracking reactions can take place. This is in accordance with theoretical expectation

$$j_{\mathrm{MTC}} \propto \frac{N}{L^2} \tag{12}$$

for the BrS topology [13].

For the MTC system, Fig. 8b, we observe a similar logarithmic increase in the maximal current with respect to c but over a smaller range of lower values of c. The current approaches the asymptotic value $j^*(c)$ faster as compared to the REF system. For $L = 1$, the range of c over which the MTC currents are higher than the REF currents is small. The range increases with N and toward lower values of c. For $L = 2, 3$, the MTC currents are higher than the REF currents almost over the entire range of c for $N \geqslant 5$. This implies the existence of MTC effect for larger ranges of c as N and L take larger values.

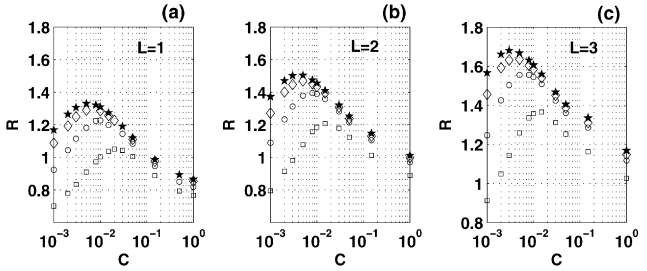

Fig. 9. Efficiency ratio R for $L = 1, 2, 3$ for system defined in Fig. 8 for $N = 3$ (□), $N = 5$ (○), $N = 7$ (◇), and $N = 9$ (★).

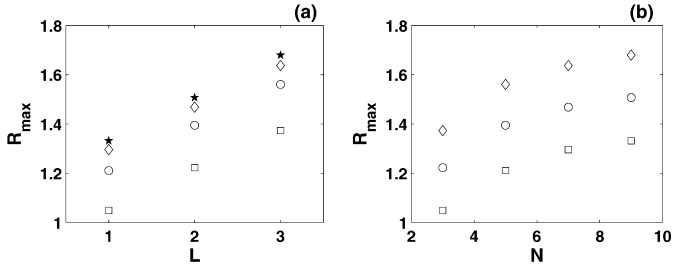

Fig. 10. The maximal efficiency ratio $R_{\max}$ for increasing values of L (a) ($N = 3$ (□), $N = 5$ (○), $N = 7$ (◇), and $N = 9$ (★)) and for increasing values of N (b) ($L = 1$ (□), $L = 2$ (○), and $L = 3$ (◇)) for system parameters defined in Fig. 8.

The efficiency ratio R (Eq. (11)) is plotted in Fig. 9 for the same parameters as in Fig. 8. The tendency of the maximal current to saturate faster with respect to c in the MTC system as compared to the REF system is shown as a decrease in R as c is increased. The efficiency ratio R rises above unity only over a short range of c for $N = 3$, $L = 1$ (Fig. 9a). However, for larger values of L, R is above unity over almost the entire range of c for $N \geqslant 5$ (cf. Figs. 9b and 9c). We also note that R increases with L and in our case, for $N = 9$, $L = 3$, $R \approx 1.68$, indicating that the MTC lattice generates 68% more current than the REF system. However, it should be noted that the absolute current in both the systems decrease with L almost by factor 3 as is seen from Fig. 8. The results nevertheless indicate a significant MTC effect particularly for larger lattices and longer channels between intersections, measured in terms of L. Although the MTC effect is more noticeable for larger N and L, it seems to saturate as N is increased. Further, $R_{\max}(c)$ shifts toward somewhat lower values of c as both N and L are increased.

The maximal value of R, $R_{\max}$ is shown in Fig. 10. Fig. 10a shows $R_{\max}$ for $L = 1, 2, 3$ and $N = 3, 5, 7, 9$. $R_{\max}$ exhibits linearity. This is in agreement with the theoretical prediction [13]

$$R_{\mathrm{BrS}} \propto L \tag{13}$$

for all values of N, as opposed to $R \sim L/N$ for the NBK topology [11]. However, for any given L, although $R_{\max}$ increases, it shows a saturation tendency. This is emphasized well in Fig. 10b, where the saturation of $R_{\max}$ is clearly seen.

3.3.2. $D_A \neq D_B$

We now turn our attention to the study of MTC effect by varying D_B. The diffusion rates of the molecules in the zeolite

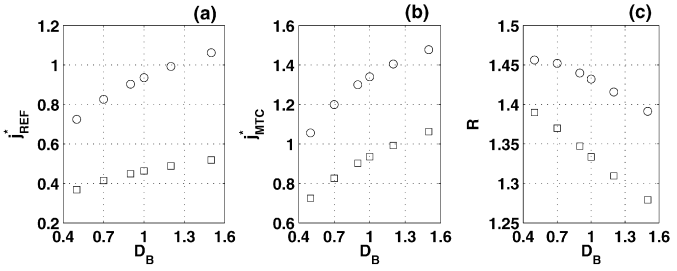

Fig. 11. Maximal currents for REF (a), MTC (b), and efficiency ratio R (c) as a function of D_B for $N = 5$ (□) and $N = 9$ (○) for $D_A = 0.5$, $c = 0.01$.

depend on temperature, size of the molecule, pore size, loading, etc. [16]. The dependence of diffusion rates of hydrocarbons on the number of carbon atoms are also reported [18,19]. The rates can decrease for larger molecules by orders of magnitude. However, when the reactant molecules contain a small number of carbon atoms, experimental evidence shows that the diffusion coefficients of the cracked molecules are higher by some numerical factor than those of the reactants [19]. Nevertheless it is necessary to study the effect of D_B on reactivity. We assume the diffusion rates of the product particles to be of the same order as that of the reactant particles. We also assume that the diffusion rates of the product particles are higher than those of the reactant particles due to their smaller size. This assumption is justified although there are reports that the particle mobility increases when its size approaches that of the pore size [20].

To test the role of D_B in enhancement of reactivity, we simulated the system for several values of D_B. We have simulated the systems for $N = 5$ and $N = 9$ and $L = 2$ by keeping $D_A = 0.5$ throughout for $c = 0.01$. We have chosen this value of c as the efficiency ratio decreases for values larger than this. The results are shown in Fig. 11. As in the earlier results, current for both REF and MTC systems increase with N. The current in both the REF and MTC systems show an increase with D_B as expected from the mobility of B-particles. However, the efficiency ratio is found to decrease for $D_B > D_A$.

We can compare these results with the case of one intersection, Fig. 6. There, as D_B is increased, an increase in R is seen for low values of D_B. But as D_B is increased, there is a monotonic decrease in R. For the case of $N = 5, 7$ in Fig. 11, we find a monotonic decrease in R as D_B is increased. However, both for one intersection and for larger lattices, R is always above unity indicating the presence of the MTC effect. But for larger lattices the maximum R is found in the region $D_A \approx D_B$. This may indicate that for the MTC system to be most effective, the mobilities of both the reactant and product particles should be nearly the same.

4. Conclusions

Our simulations show that there is a significant MTC effect for the cracking reaction in the BrS topology with size selectivity. Rather than studying a specific reaction with given numerical values for the diffusivities and reaction constants we have performed a parametric study for an idealized cracking reaction $A \to 2B$ with identical reaction products on a wide range of reaction rates and diffusivities. It turns out that the strength of the MTC effect depends on the ratios $D_{A,B}/c$ of the particle diffusivities and reaction constant. We find both for the REF and MTC systems that the output current of B-particles which describes the molecular outflow of reaction products tends to saturate as c is increased. However, the asymptotic value is reached in MTC system for lower values of c than that in the REF case. The effectiveness of MTC also seems to be more pronounced when the reactant and product diffusivities are closer, i.e., $D_A/D_B \approx 1$.

The MTC effect also improves for larger lattices and larger channel segments between intersections, but the efficiency ratio saturates. The earlier analytical treatment of an isomerization reaction $A \to B$ for similar pore topology [13] suggests that this trend continues with increasing lattice size. Hence, even though our simulations are performed on very small lattices we may conclude that unlike as in the NBK topology [11], the MTC effect in the BrS topology persists for large commercially-sized grains.

In our treatment, the dynamics is a combination of both exclusion and nonexclusion dynamics since reactants and products are assumed to be of different size. A comparison of observations between this study and a similar study for the isomerization process on the same topology has been made [13]. In the isomerization case reactants and products are considered to be of equal size and full mutual exclusion was postulated. The observations are qualitatively similar in both models, which implies that the topology has a greater role than the particular reaction or the dynamics under consideration.

We have attempted in this work to determine the effectiveness of MTC over the REF system on a model two-dimensional lattice network with a small number of channels. We have chosen the simple BrS channel topology as it allows for fairly fast simulation while still capturing the salient features of a potentially successful MTC-topology. It is too early to judge how strong precisely an MTC effect could be in real materials as it may depend on various microscopic features of the interactions among molecules inside a pore and with pore walls and also on the precise dynamical details of the exchange with the gas phase. As a next step it would be interesting to study the effectiveness of MTC for real three-dimensional channel topologies. An interesting candidate is the three-dimensional bimodal structure of TNU-9 [14]. Simulation of this topology requires much higher numerical effort, but appears to be feasible, and will provide insight in the importance of the details of the channel topology.

Acknowledgment

The authors acknowledge financial support by the Deutsche Forschungsgemeinschaft within the priority programme SPP 1155.

References

[1] M. Boronat, P. Viruela, A. Corma, Phys. Chem. Chem. Phys. 3 (2001) 3235.

[2] G. Yaluris, R.J. Madon, D.F. Rudd, J.A. Dumesic, Ind. Eng. Chem. Res. 33 (1994) 2913.
[3] S.V. Nedea, A.P.J. Jansen, J.J. Lukkien, P.A.J. Hilbers, Phys. Rev. E 65 (2002) 066701.
[4] J. Kärger, F. Stallmach, in: P. Heitjans, J. Kärger (Eds.), Diffusion in Condensed Matter, Springer, Berlin, 2005, p. 434.
[5] E.G. Derouane, Z. Gabelica, J. Catal. 65 (1980) 486.
[6] E.G. Derouane, Appl. Catal. A 115 (1994) N2.
[7] N. Neugebauer, P. Bräuer, J. Kärger, J. Catal. 194 (2000) 1.
[8] J. Kärger, P. Bräuer, H. Pfeifer, Z. Phys. Chem. (Munich) 104 (2000) 1707.
[9] J. Kärger, P. Bräuer, A. Neugebauer, Europhys. Lett. 53 (2001) 8.
[10] A. Brzank, G.M. Schütz, P. Bräuer, J. Kärger, Phys. Rev. E 69 (2004) 031102.
[11] A. Brzank, G.M. Schütz, Appl. Catal. A 288 (2005) 194.
[12] A. Brzank, S. Kwon, G.M. Schütz, Diffus. Fundam. 1 (2005) 1.
[13] A. Brzank, G.M. Schütz, J. Chem. Phys. 124 (2006) 214701.
[14] F. Gramm, C. Baerlocher, L.B. McCusker, S.J. Warrender, P.A. Wright, B. Han, S.B. Hong, Z. Liu, T. Ohsuna, O. Terasaki, Nature 444 (2006) 79.
[15] D. Theodorou, J. Wei, J. Catal. 83 (1983) 205.
[16] F.J. Keil, R. Krishna, M. Coppens, Rev. Chem. Eng. 16 (2000) 71.
[17] W.H. Press, S.A. Teukolsky, W.T. Vetterling, B.P. Flannery, Numerical Recipes in FORTRAN, Cambridge Univ. Press, Cambridge, 1993, p. 272.
[18] R. Tsekov, P.G. Smirniotis, J. Chem. Phys. B 102 (1998) 9385.
[19] F. Leroy, B. Rousseau, Mol. Sim. 30 (2004) 617.
[20] E.G. Derouane, J.M. Andre, A.A. Lucas, J. Catal. 110 (1988) 58.